REVISION

27th August 2016

---

# Electrothermal Annealing of Catalytic Platinum Microwire Electrodes: Towards Membrane-Free pH 7 Glucose Micro-Fuel Cells

---

James Weber [1], Andrew J. Wain [2],
Gary A. Attard [3], and Frank Marken *[1]

[1] *Department of Chemistry, University of Bath, Claverton Down, Bath BA2 7AY, UK*
[2] *National Physical Laboratory, Teddington, United Kingdom, TW11 0LW, UK*
[3] *Department of Physics, The Oliver Lodge Laboratory, University of Liverpool, Oxford Street, Liverpool L69 7ZE, UK*

**To be submitted to Electroanalysis (Special issue ESEAC 2016)**

Proofs to F. Marken

Email F.Marken@bath.ac.uk

## Abstract

Surface activation and cleaning of platinum micro-wires of 25 micron diameter has been achieved by a short one-second electrothermal annealing treatment in air at 0.3 A (to orange glow). Voltammetric data suggest a decrease in the electrochemically active surface area with annealing time and a change in surface structure towards the Pt(100) crystalline face. The impact of electrothermal annealing on the electrocatalytic activity towards (i) oxygen reduction and (ii) glucose oxidation in pH 7 phosphate buffered aqueous solutions is investigated. In contrast to as-received platinum, annealed platinum produces an electrocatalytic response towards glucose oxidation with increasing glucose concentration. A short one-second anneal step is just as effective in enhancing catalysis as prolonged electrochemical cleaning in sulphuric acid. Finally, by combining a non-annealed and an annealed microwire electrode, a very simple membrane-free micro-fuel cell system is devised operating in phosphate buffer at pH 7 with linearly increasing power output reaching 2.2 nW $cm^{-2}$ for high glucose levels of 0.5 M.

**Keywords:** microwire electrode, voltammetry, electrothermal annealing, glucose oxidation, sensor.

**Graphical Abstract:**

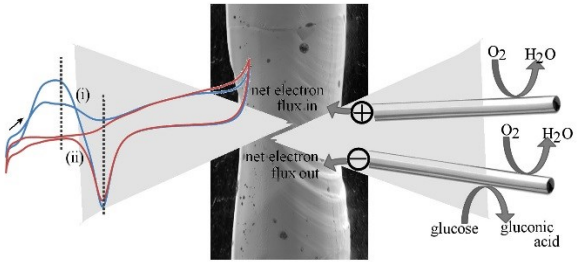

## 1. Introduction

Platinum has been employed in many areas of electrochemistry and in particular those involving catalytic energy conversion and sensing. Electrochemical power generation from "bio-fuels" such as glucose [1], ammonia [2], alcohols [3], or cellulose [4] plays an important role in sensing applications or in micro-power sources to supply electrical energy to implantable devices [5] and micro-devices [6]. Normal, healthy physiological levels of glucose in human blood fall into the range of 4 to 6 mM and at lower levels glucose is also present in tissue and other bio-fluids [7]. The generation of power by electrochemical oxidation of this concentration of glucose to carbon dioxide (associated with the 4-electron reduction of oxygen to water) should deliver theoretically in the order of 1 mW $cm^{-2}$ power, but the experimentally achieved values are highly dependent on suitable enzyme catalysts and device design [8]. Often enzymes are employed to allow effective and selective reactions at the anode and cathode to occur. With highly specialised bio-catalysts or well-engineered mass transport conditions membrane-free micro-fuel cells are possible with very limited fuel cross-over [9]. However, incorporation of bio-catalysts into devices remains problematic and simple catalytic surfaces may offer a desirable alternative.

Platinum microwire electrodes have been widely studied [10,11,12] and employed, for example, in sensing [13]. The diffusion to mirowire electrodes is cylindrical and rapidly approaches quasi-steady state [14], which helps in stabilising sensor responses. Hence, the application of microwires as fuel cell electrodes has potential benefits in terms of stability of power output and has been employed, for example, in PtCu alloy electrocatalyst testing [15]. In this report, we present a rapid method of cleaning and annealing commercial platinum microwires using electrothermal treatment. Similar to

the more common "flame annealing" methods, that are commonly applied for example in the preparation of platinum electrodes for oxygen reduction [16,17], the electroannealing method can be applied reproducibly and conveniently. It is shown that platinum can be made more active towards the oxidation of glucose in pH 7 phosphate buffer media and that a combination of two microwires, one annealed and one not, immersed into the same solution can be employed to generate power.

## 2. Experimental Details

### *2.1. Chemical Reagents*

Phosphoric acid ($H_3PO_4$, 85 %), sulphuric acid ($H_2SO_4$, 95-98 %), sodium hydroxide (NaOH, 98 %), D-(+)-glucose and hydrochloric acid (HCl, stabilised at 1 M) were obtained from Sigma Aldrich UK. Commercial platinum wire of 25 μm diameter was purchased from Advent Materials UK. All chemicals were used as received without further purification. Solutions were prepared using purified water with a resistivity of not less than 18 MΩ cm at 22 $^{o}$C. Aqueous 0.1 M phosphate buffer solutions were prepared to pH 7. Argon gas was purchased from BOC UK (Pureshield).

### *2.2. Instrumentation*

Electrochemical experiments were carried out using a three-electrode configuration in a custom-made glass cell, using a KCl-saturated calomel reference (SCE) electrode, a platinum wire counter electrode and a laminated 25 μm diameter platinum microwire as the working electrode prepared as reported previously [14]. Leakage of chloride form the SCE reference into the measurement cell was observed to significantly affect results and therefore electrolyte solution was frequently renewed. Electrochemical

measurements were performed using an Ivium Compactstat (Netherlands) at room temperature, 22 ± 1 $^{o}$C. Electrothermal annealing of the microwire electrodes were performed using an ISO-Tech IPS1603D power source. Copper tape was applied to the end of wires to improve connections (Figure 1). If not stated otherwise, all solutions were purged for 10 minutes using Ar gas prior to performing electrochemical measurements. Scanning electron micrographs were obtained on a JEOL JSM6310 SEM.

### *2.3. Procedures I.: Electrode Fabrication and Annealing*

Fabrication of the microwire electrodes was carried out according to a previously reported method [14], using 25 μm diameter platinum wire and commercial lamination foil with an individual sheet thickness of 125 μm. Electrothermal annealing of the platinum microwires was achieved by passing a current of 0.3 A (to give orange glow or approximately ~1000 K) through a set length wire of approximately 6 cm for either 1 s, 10 minutes, or 4 h before lamination and use in experiments. Electrochemical cleaning of the platinum microwires was achieved by potential cycling at with a scan rate of 0.5 V $s^{-1}$ from -0.5 to +1.3 V vs. SCE for 35 cycles in aqueous 0.5 M $H_2SO_4$.

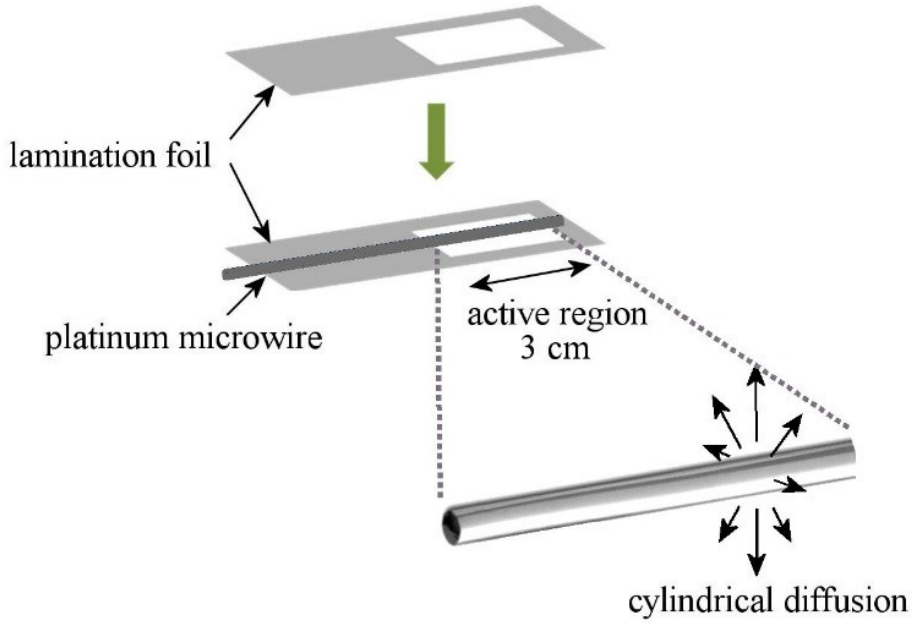


**Figure 1.** Schematic drawing of the assembly of the platinum microwire (after annealing) into lamination foil to allow a 3 cm long section to be exposed to solution.

### *2.3. Procedures II.: Glucose Micro-Fuel Cell Fabrication*

A glass cylinder of length 3 cm and internal diameter of approximately 5 mm was prepared from a glass pipette. The as-received platinum microwire and the electrothermally annealed (at 0.3 A for 1 s) platinum microwire were attached to the inside of the glass cylinder at opposite sides using silicone sealant (Ambersil, Silicoset 150). The bottom of the glass cylinder was then was sealed and solution were filled in to 2 cm height. A potentiostat was employed to read out point-by-point the steady state current as a function of applied potential.

## 3. Results and Discussion

***3.1. Effects of Electroannealing on Surface Area and Faceting.*** The characterisation of commercial platinum wire before and after electrothermal annealing was first carried

out using scanning electron microscopy imaging (SEM). The commercial platinum wire (Figures 2A,B) displays a rough surface morphology with vertical crevices all following the same direction along the wire, that were likely formed from the mechanical process during production (temper hard, 99.99%). After electrothermal annealing at 0.3 A for 1 s (see Figures 2C and 2D), smooth surface features are observed along with crystal outline or “step” like features, indicating the formation of larger atomic terraces of lower surface energy and the progression towards a more monocrystalline structure. This trend is very clear for 4 h annealed samples (Figure 2E and 2F). By comparison, simple electrochemical cleaning by potential cycling did not significantly affect the morphology, at least at the micrometer scale. Dark spots seem to be associated with areas where impurities segregate.

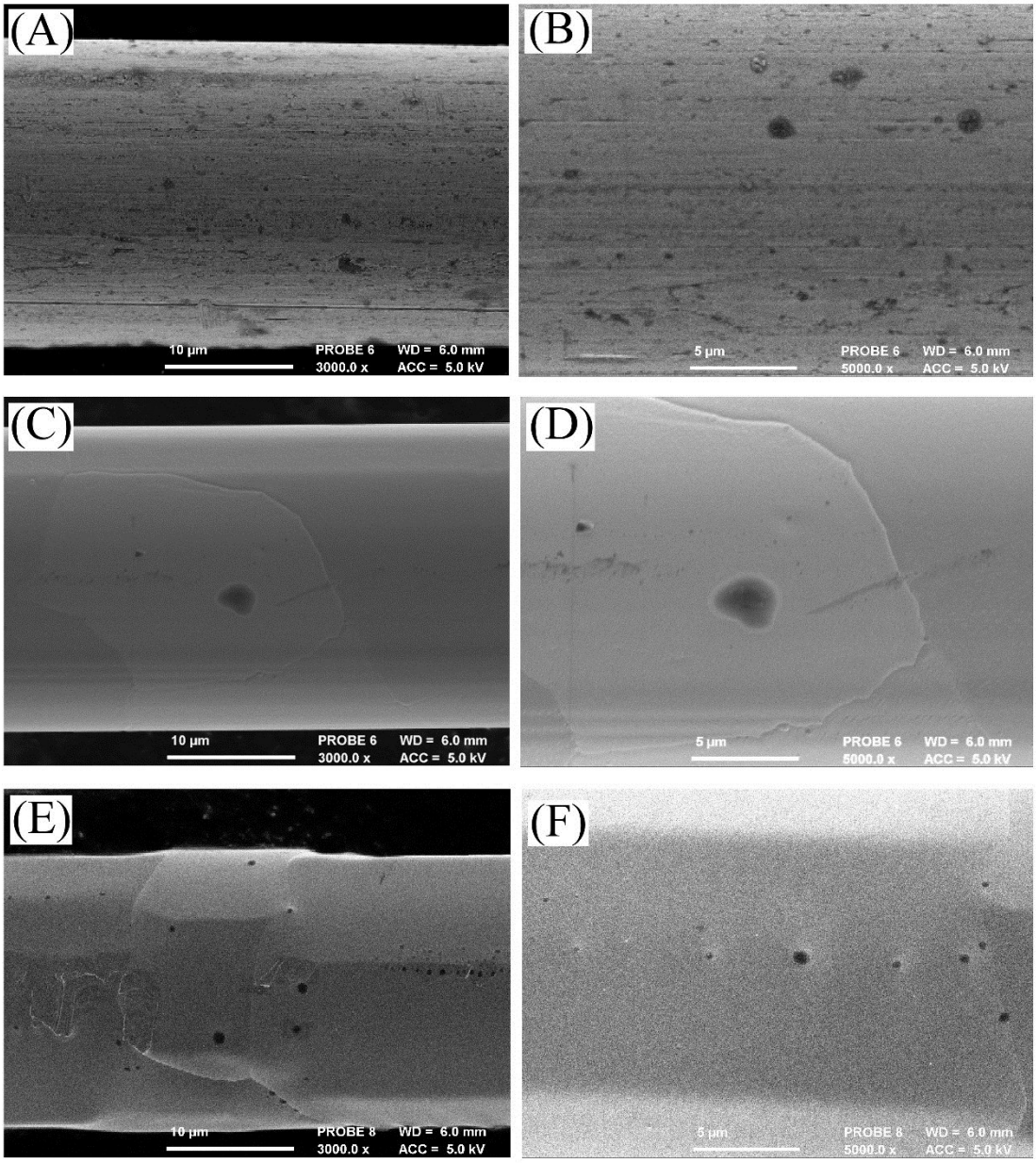


**Figure 2.** Scanning electron micrographs (SEMs) of (A,B) a commercial platinum wire (temper, hard), (C,D) a 1 s electrothermally annealed, and (E,F) a 4 h electrothermally annealed platinum wire (annealing current 0.3 A over 6 cm length).

Electrochemical characterisation of the commercial platinum wire before and after electrothermal annealing at 0.3 A for 1 s was conducted in 0.5 M $H_2SO_4$ (Figure 3). Voltammetric data for a platinum wire that has been electrochemically cleaned by voltammetric cycling is also shown. All three wires exhibit characteristic poly-

crystalline platinum features in acid, with platinum surface oxidation (between ca. 0.40 V and 1.25 V vs. SCE) and the hydrogen underpotential deposition (HUPD) region (between ca. 0.10 V and -0.25 V vs. SCE) clearly observed. The pair of peaks at ca. -0.15 V vs. SCE are associated with Pt (110) sites (or more accurately, defects that are the junction of two (111) planes, i.e. (111)×(111), which is actually equivalent to a "(110)" step), whilst those at ca. -0.10 V vs. SCE indicate Pt (100) (or more accurately, defect sites due to the junction of a (111) and (100) plane, i.e. (111)×(100) steps) [18,19,20].

After electrothermal annealing for 1 s, three observations are evident: (i) the total current associated with HUPD has decreased, (ii) the Pt (111)×(100) signal has become more predominant over the Pt (111)×(111) signal and (iii) there is a feature just positive of the (111)×(100) sites from 0.0 to 0.15 V vs. SCE that can be identified as being associated with (100) sites. The electrochemical cleaning of the as-received wire has the effect of increasing the sharpness of the HUPD peaks, indicative of removal of contaminants. The electrochemically cleaned sample also has a much smaller population of (100) sites but still significant (111)×(100) steps, consistent with all terrace order being disrupted by potential cycling into the oxide region.

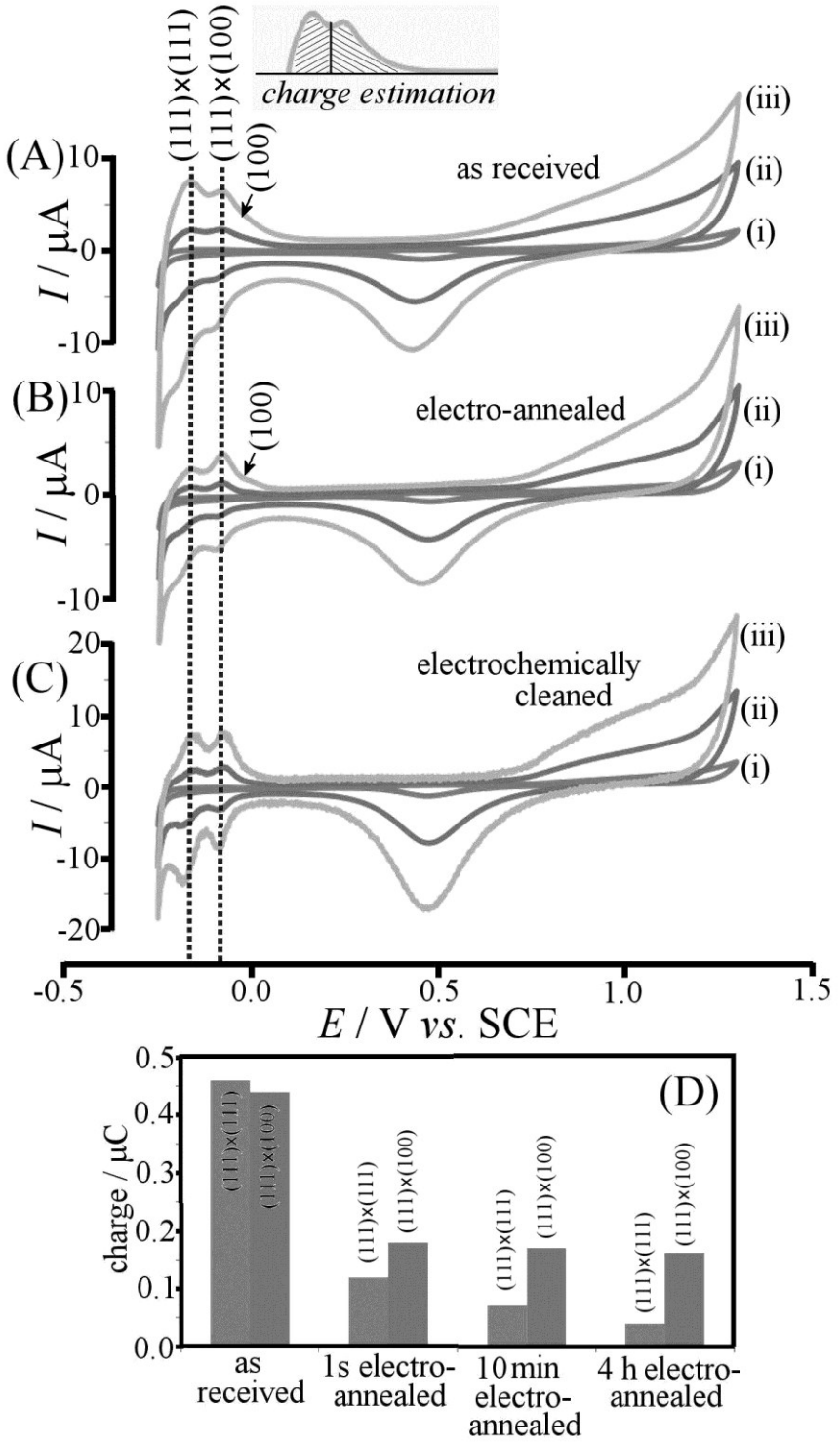


**Figure 3.** Cyclic voltammograms (scan rate (i) 20, (ii) 200 and (iii) 500 mV $s^{-1}$; in 0.5 M $H_2SO_4$ under argon) for a 25 μm diameter platinum microwire (A) as received, (B) after electrothermal annealing at 0.3 A for 1 s, and (C) electrochemically cleaned for 35 cycles in 0.5 M $H_2SO_4$. The inset shows how the charge under the peak was estimated. (D) Bar graph of the estimated charge from electrochemical measurements of $Q_H$ for Pt(111)×(111) and $Q_H$ Pt (111)×(100) for increasing annealing times.

Integrating the charge under the curve (capacitive background-subtracted; with approximate peak delimiters; see inset Figure 3) for the HUPD regions associated with the Pt(111)×(111) and Pt(111)×(100) sites, and using the corresponding approximate conversion factors (210 μC $cm^{-2}$ [21]), it is possible to estimate the active electrochemical area (ESA) of the platinum wire as a function of associated crystallographic plane (Table 1; Figure 3D). However, the geometric surface area for a 25 μm diameter wire of 3 cm length is expected to be 2.3 $mm^2$, which suggests that values obtained here are somewhat low, possibly due to a fast RC time constant for the microware electrode and/or insufficient time resolution of the digital potentiostat system. Furthermore, due to the convolution of the adsorption/desorption peaks in the HUPD region the absolute values for charge associated with Pt(111)×(111) and Pt(111)×(100) are not accurate. However, the approximate ratio of Pt(111)×(100) to Pt(111)×(111) charges provides a useful indication of the relative changes in surface structure as a result of the annealing process.

**Table 1.** Estimated electrochemical charge and surface area data (from cyclic voltammetry data at 500 $mVs^{-1}$ in 0.5 M $H_2SO_4$; ESA; assuming $H_{ads}$ is 210 μC/$cm^2$ [19]) for increasing annealing time at 0.3 A of a commercial platinum wire compared to electrochemical cleaning in aqueous 0.5 M $H_2SO_4$.

| | **Charge under $H_{ads}$ region / μC** | **Charge under Pt(111) ×(111) / μC** | **Charge under Pt(111) ×(100) / μC** | **Ratio Q(111)× (100) / Q(111)× (111)** | **Charge under ($PtO_x$/PtOH) / μC** | **Ratio $Q_O/Q_H$** | **ESA / $mm^2$** |
|---|---|---|---|---|---|---|---|
| **Electro-chemically cleaned Pt** | 1.08 | 0.44 | 0.64 | 1.4 | 7.1 | 6.6 | 0.51 |
| **Pt wire as received** | 0.90 | 0.46 | 0.44 | 0.96 | 6.8 | 7.6 | 0.43 |
| **0.3 A 1 s** | 0.30 | 0.12 | 0.18 | 1.5 | 4.2 | 14 | 0.14 |
| **0.3 A 10 min** | 0.24 | 0.07 | 0.17 | 2.4 | 4.0 | 16 | 0.11 |
| **0.3 A 4 h** | 0.20 | 0.04 | 0.16 | 4.0 | 3.8 | 19 | 0.09 |

With increasing annealing time, (i) the ratio of Pt(111)×(100) to Pt(111)×(111) appears to increase and (ii) the total electrochemically active surface area (ESA) appears to decrease. It is evident that applying a high current through the wire (to generate orange glow) provides enough thermal energy for significant atomic restructuring of the surface (and bulk) and the energetically favoured Pt(100) crystallographic plane to dominate (either as steps or in the form of terraces). With increasing annealing time, single crystalline regions begin to form, resulting in loss of ESA and causing the microwire to become more brittle.

***3.2. Effects of Electroannealing on Glucose Oxidation.*** Voltammetric data for the oxidation of glucose was obtained in 0.1 M phosphate buffer at pH 7 and under argon using (A) an as-received platinum microwire, (B) an electrothermally annealed microwire, and (C) an electrochemically cleaned microwire (Figure 4). The oxidation of glucose is detected as anodic current signal with onset at -0.46 V vs. SCE very close to the hydrogen adsorption region. For the as-received platinum wire there is no significant oxidation for glucose even with increasing glucose concentrations. This indicates that there is little or no catalytic activity, possibly due to adsorbed species blocking the sites required for glucose oxidation.

After electrothermal annealing at 0.3 A for 1 s, a glucose oxidation signal is clearly observed (Figure 4B). The action of thermal annealing for 1 s is enough to burn away any contaminates and adsorbed species to leave behind a clean, active surface. Furthermore, it is known that the Pt(100) surface is the most active toward glucose

oxidation [22], which is enhanced after electrothermal annealing. A similar effect is observed for the electrochemically cleaned platinum microwire electrode (Figure 4C) where a comparable activity for glucose oxidation is observed. This is an interesting observation in that the ESA of the electrothermally annealed wire is approximately four times smaller than the electrochemically cleaned wire, which suggests a trade-off between increasing site-specific activity and decreasing total surface area.

Chloride anions have been shown to compete with the binding of glucose on reactive platinum surfaces. Chloride therefore often acts as inhibitor for glucose oxidation except for processes at some modified platinum materials [23]. Figure 4D demonstrates the dramatic effect of the addition of 0.1 M NaCl into the solution. The glucose oxidation signal is immediately suppressed and so the oxidation of glucose prevented. When using the SCE reference electrode this effect also needs to be considered and indeed small leaks over time of chloride anions into solution with glucose can partially suppress the electrocatalytic response.

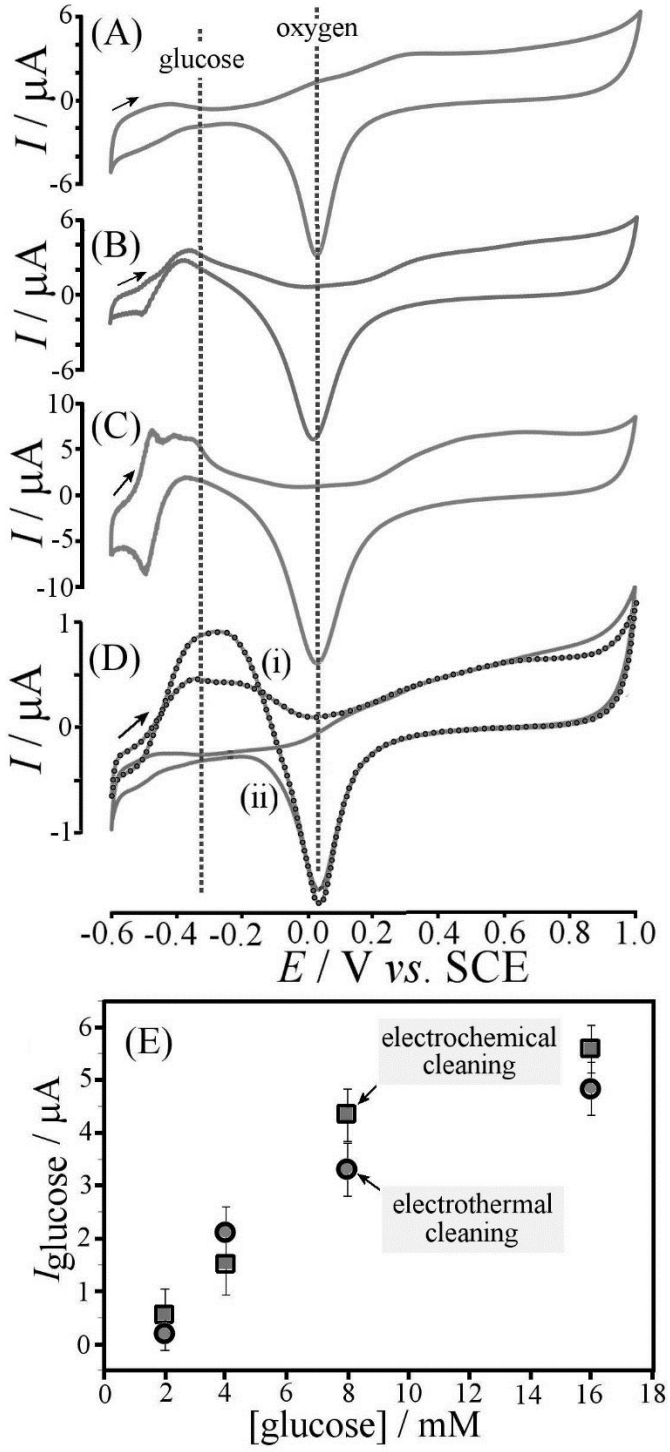


**Figure 4**. (A-C) Cyclic voltammograms (scan rate 200 $mVs^{-1}$) for oxidation of 4 mM glucose in 0.1 M phosphate buffer pH 7 using (A) an as-received platinum microwire (B) an electrothermally annealed platinum microwire (0.3 A, 1 s), (C) an electrochemically cleaned platinum microwire (after 35 cycles at 500 mV $s^{-1}$ in 0.5 M $H_2SO_4$). (D) Comparison of cyclic voltammograms (scan rate 20 $mVs^{-1}$) for oxidation of 4 mM glucose at an electrothermally annealed platinum microwire (0.3 A, 1 s) in the absence (i) and in the presence (ii) of 0.1 M NaCl. (E) Plot of glucose oxidation peak current (scan rate 200 $mVs^{-1}$) versus glucose concentration for two types of electrodes (error bars calculated from an average of three repeats).

The inhibition effects of chloride poisoning on platinum can be partially avoided by increasing the scan rate. At a scan rate of 20 mV $s^{-1}$ the signal for glucose oxidation is reduced significantly, but when increasing the scan rate to 200 mV $s^{-1}$ an increase in the glucose oxidation signal is achieved by out-running the competing adsorption of chloride anions on to the platinum surface. The similarity in reactivity of the 1 s electrothermally annealed electrode and the electrochemically cleaned electrode can be demonstrated when comparing the glucose oxidation current as a function of glucose concentration. Figure 4E shows a plot with both types of electrodes showing increasing current versus glucose concentration and beginning to plateau at approximately 10 mM. Although it is clear that electrochemical cleaning and electrothermal annealing are equally beneficial in terms of improving the catalytic activity of as-received Pt microwires, the protocol for the electroannealing process is fast and convenient when compared to the electrochemical cleaning process in sulfuric acid.

***3.3. Effects of Electroannealing on Oxygen Reduction.*** The reduction peak signal at +0.02 V vs. SCE (Figure 4) is associated mainly with the conversion of surface oxidised platinum species back to platinum metal. However, at similar potentials the reduction of oxygen can also be observed. Figure 5 shows voltammetric data comparing (A) an as-received platinum microwire, (B) an electrothermally annealed, and (C) an electrochemically cleaned microwire electrode in 0.1 M phosphate buffer with ambient levels of oxygen (ca. 0.2 mM). The reduction peak appears increased when compared to data in Figure 4 and for voltammetric signals recorded at slower scan rate a clear step-feature consistent with the steady reduction response for oxygen are observed. All

three electrodes show similar peak features and mass transport-limited currents for oxygen reduction although the oxide reduction peak feature for the electrothermally annealed electrode appears to be most pronounced. Whilst a full analysis of oxygen reduction kinetics are beyond the scope of this paper, it can be concluded that (in contrast to literature data reported for sulfuric acid media [24,25]) in phosphate buffer all three electrodes appear similarly active towards oxygen reduction.

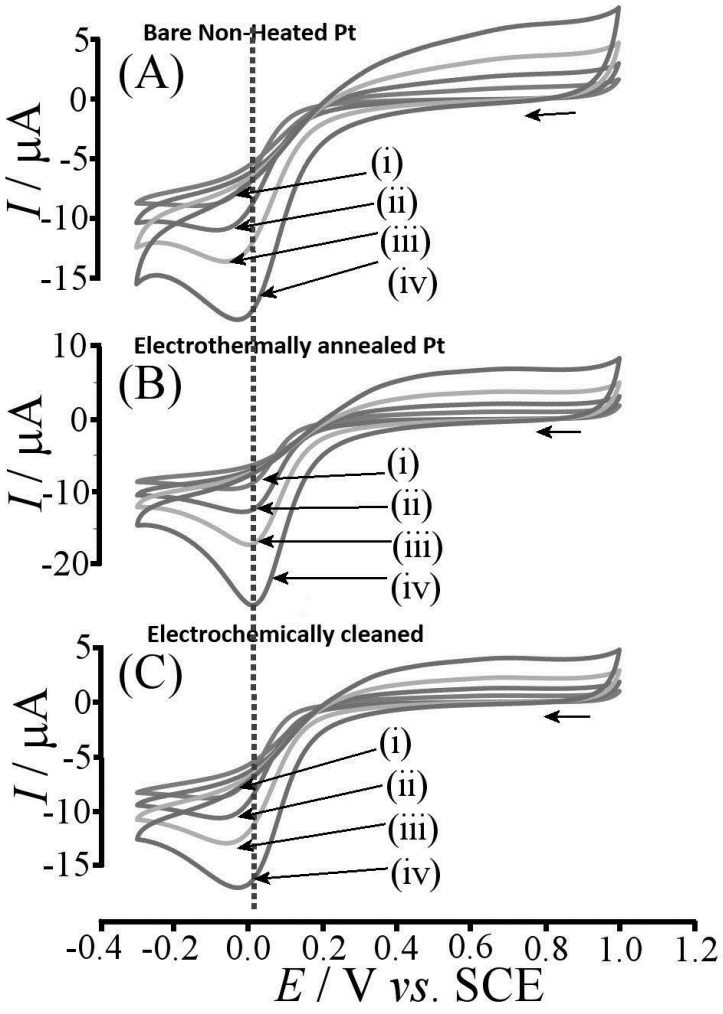


**Figure 5.** Cyclic voltammograms (scan rates of (i) 20 (ii) 50 (iii) 100 and (iv) 200 mV $s^{-1}$) for reduction of ambient oxygen in 0.1 M phosphate buffer pH 7 using (A) an as-received platinum microwire, (B) an electrothermally annealed platinum microwire (0.3 A, 1 s), and (C) an electrochemically cleaned platinum microwire (35 cycles at 500 mV $s^{-1}$ in 0.5 M $H_2SO_4$).

***3.4. Membrane-less Oxygen – Glucose Micro-Fuel Cell.*** In order exploit the differences in reactivity observed for the electrothermally annealed versus the as-received platinum microwire electrode, we investigate the spontaneous power generation of the two microwires immersed in 0.1 M phosphate buffer at pH 7 in the presence of glucose. As concluded from section 3.2, the as-received platinum electrode is not able to oxidise glucose, whilst electrothermal annealing clearly activates the electrode towards this reaction. This catalytic asymmetry coupled with the oxygen reduction activity of both electrodes results in a measurable potential difference and in practice a zero current potential of typically 90 mV is observed (Figure 6A). When varying the potential applied between the two electrodes away from the equilibrium value currents are observed. Figure 6A summarises the point-by-point measured current data and three reaction zones are clearly distinguished. At all negative potentials and at potential positive of +90 mV, current and potential exhibit opposite signs and therefore energy is consumed. Only in the middle section from 0 mV to 90 mV is a zone of energy production observed.

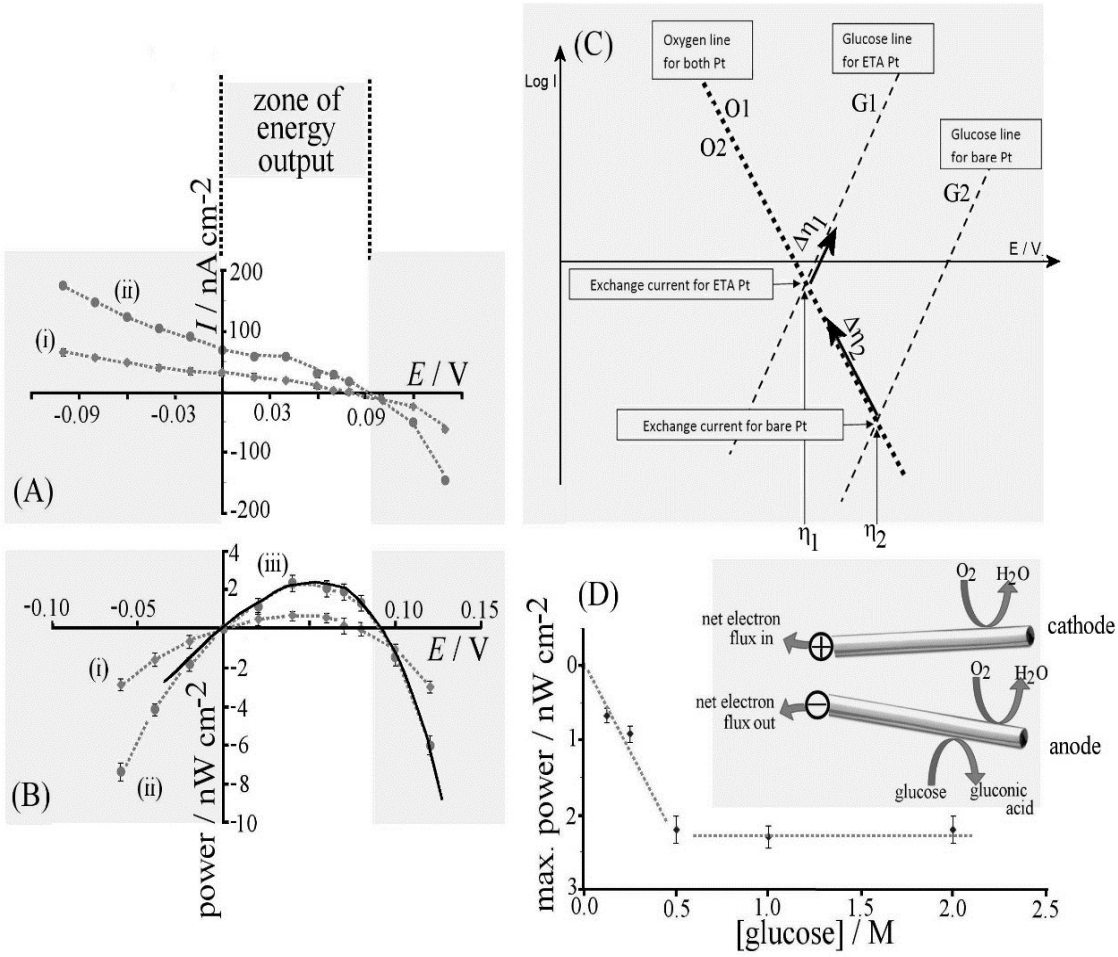


**Figure 6.** (A) Current versus potential plot for two platinum microwires (one as-received and one electroannealed for 1 s) immersed into (i) 0.125 M and (ii) 1.0 M glucose in 0.01 M phosphate buffer at pH 7 (average taken over three readings). (B) The associated power output for (i) 0.125 M and (ii) 1.0 M glucose in 0.01 M phosphate buffer at pH 7 (error bars for three repeats). Line (iii) shows a theory line based on the assumption that simple Tafel behaviour prevails (see text). (C) Schematic drawing of Tafel lines for the two platinum microwire electrodes to demonstrate the fundamental origin of the power output. (D) Variation of maximum power output at 50 mV with increasing glucose concentration in 0.01 M phosphate buffer pH 7. The inset shows a schematic drawing of the two proposed electrode reactions.

Plots of power output are shown in Figure 6B, which exhibit a maximum at approximately +50 mV. The schematic Tafel plot in Figure 6C can be used to better explain the observed behaviour. Zero current points $\eta_1$ and $\eta_2$ are indicated for the two types of electrodes (assuming similar reactivity to oxygen). The Tafel lines for oxygen

reduction at electrode 1 and 2 are denoted O1 and O2, and those for glucose oxidation are denoted G1 and G2. Current flow during power generation is indicated by two arrows associated with a change in overpotential $\Delta\eta_1$ and $\Delta\eta_2$. The magnitude of oxygen reduction current (at the as-received electrode) and the glucose oxidation current (at the electrothermally annealed electrode) need to be equal and therefore the oxygen reduction process associated with $\Delta\eta_2$ is the dominating process.

In order to compare theory and experiment more quantitatively the relevant processes indicated here as O1/O2 and G1/G2 (see Figure 6D) can be expressed under open circuit conditions in terms of the corresponding Tafel laws (equations 1-4).

$$logI_{O1} = a_{O1}(\eta_1) + b_{O1} \quad (1)$$

$$logI_{O2} = a_{O2}(\eta_2) + b_{O2} \quad (2)$$

$$logI_{G1} = a_{G1}(\eta_1) + b_{G1} \quad (3)$$

$$logI_{G2} = a_{G2}(\eta_2) + b_{G2} \quad (4)$$

The symbols *a* and *b* denote Tafel parameters. Values for $\eta_1 = \frac{b_{G1}-b_{O1}}{a_{O1}-a_{G1}}$ and $\eta_2 = \frac{b_{G2}-b_{O2}}{a_{O2}-a_{G2}}$ can be obtained from the Tafel parameters. Under conditions of power output, the currents $I_{O2}$ and $I_{G1}$ are directly associated with oxygen reduction at the as received electrode and glucose oxidation at the electrothermally annealed electrode (equations 5 and 6).

$$logI_{O2} = a_{O2}(\eta_2 - \Delta\eta_2) + b_{O2} \quad (5)$$

$$logI_{G1} = a_{G1}(\eta_1 + \Delta\eta_1) + b_{G1} \quad (6)$$

The balance of currents between anode and cathode can now be expressed as $I_{O2} - I_{O2}^{0} = I_{G1} - I_{G1}^{0}$, where the superscript 0 is used to indicate zero net current conditions with $\Delta\eta_1 = \Delta\eta_2 = 0$. Although the resulting equation cannot be solved analytically, it is possible to express $\Delta\eta_1$ as a function of $\Delta\eta_2$ (equation 7).

$$\Delta\eta_1 = \frac{1}{a_{O1}} log\left[10^{a_{G2}(\eta_2 - \Delta\eta_2) + b_{G2}} - 10^{b_{G2}} + 10^{b_{O1}}\right] \quad (7)$$

It is then possible to calculate the potential difference between anode and cathode as $\Delta E = (\eta_2 - \Delta\eta_2) - (\eta_1 + \Delta\eta_1)$. The corresponding current is obtained either from equation 5 or 6. The behaviour of the theoretical output is dominated by the oxygen reduction kinetics (as shown in Figure 6C) and $\Delta\eta_2$ has to be significantly higher compared to $\Delta\eta_1$. With realistic values (i.e. a Tafel slope of 118 mV for oxygen reduction and 59 mV for glucose oxidation) and adjusting the *b* constants (here $b_{O1} = b_{O2} = b_{G1} = -6.5$ and $b_{G2} = -8.8$) to match the experimentally observed 90 mV open circuit potential, a good match of theory and experiment is achieved (see power plot in Figure 6B). From this it can be concluded that in aqueous 1.0 M glucose in 10 mM phosphate buffer pH 7 the rate for glucose oxidation at "as-received" platinum is 33 time slower compared to that at electroannealed platinum. This result is consistent with data observed with voltammetry (see Figure 4A and 4B).

Figure 6D shows the maximum power output as a function of glucose concentration and it can be observed that a plateau is reached with 2 nW $cm^{-2}$ at ca. 0.5 M glucose probably indicative of saturation of the catalyst surface. Improvements of this system may be possible by changing the relative area of anode and cathode and by further

modifying the catalytic behaviour (e.g. Tafel parameters). For realistic devices the effects of catalyst poisoning would also need to be considered.

## 4. Summary and Conclusion

A simple electro-annealing cleaning procedure has been devised to rapidly clean a platinum microwire. Based on voltammetric data, a one-second treatment has been shown to be as effective as prolonged potential cycling in sulfuric acid, although the electrochemically active surface area (ESA) and surface structure also changed significantly during electrothermal treatment. Nevertheless, good electrocatalytic activity towards glucose oxidation in pH 7 phosphate buffer is observed and a very simple "membrane-free" micro-fuel cell concept has been proposed based on a combination of an as-received and an electro-annealed platinum microwire. Differences in reactivity cause a net glucose oxidation process at the electro-annealed microwire anode and a net oxygen reduction process at the as-received platinum microwire cathode. Due to excess glucose in the solution the energy penalty of removing oxygen at the anode can be accepted and the energy output can be shown to be proportional to glucose levels. The power versus potential profile has been shown to be dominated by the oxygen reduction kinetics. Realistically, for practical applications better catalysts are required and poisoning of the platinum (for example by chloride and proteins) would have to be taken care of and the power output would have to be significantly improved.

## Acknowledgements

J.W. and A.J.W acknowledge the financial support of the UK National Measurement System. We thank John M. Mitchels and Ursula Potter for help with electron microscopy.

## References

[1] M. Zhou, *Electroanalysis*, **2015**, *27*, 1786-1810.

[2] C. Zhong, W.B. Hu and Y.F. Cheng, *J. Mater. Chem. A*, **2013**, *1*, 3216-3238.

[3] A. Kundu, J.H. Jang, J.H. Gil, C.R. Jung, H.R. Lee, S.H. Kim, B. Ku and Y.S. Oh, *J. Power Sources*, **2007**, *170*, 67-78.

[4] H.A. Sedky, Y.S. Kim and S.E. Oh, *Enzyme Microbial Technol.*, **2012**, *51*, 269-273.

[5] Y.H. Joung, *Internat. Neurol. J.*, **2013**, *17*, 98-106.

[6] J.D. Morse, *Internat. J. Energy Res.*, **2007**, *31*, 576-602.

[7] K.H. Cha, Y. Qin and M.E. Meyerhoff, *Electroanalysis*, **2015**, *27*, 670-676.

[8] M. Falk, Z. Blum and S. Shleev, *Electrochim. Acta*, **2012**, *82*, 191-202.

[9] M.N. Nasharudin, S.K. Kamarudin, U.A. Hasran and M.S. Masdar, *Internat. J. Hydrogen Energy*, **2014**, *39*, 1039-1055.

[10] K. Aoki, K. Honda, K. Tokuda and H. Matsuda, *J. Electroanal. Chem*. **1985**, *182*, 267-279.

[11] D. Omanovic, C. Garnier, K. Gibbon-Walsh and I. Pizeta, *Electrochem. Commun.*, **2015**, *61*, 78-83.

[12] E. Espada-Bellido, Z.S. Bi and C.M.G. van den Berg, *Talanta*, **2013**, *105*, 287-291.

[13] J. Ellison, C. Batchelor-McAuley, K. Tschulik and R.G. Compton, *Sens. Actuators B-Chem*. **2014**, *200*, 47-52.

[14] J. Weber, A.J. Wain and F. Marken, *Electroanalysis*, **2015**, *27*, 1829-1835.

[15] H.J. Qiu, X. Shen, J.Q. Wang, A. Hirata, T. Fujita, Y. Wang and M.W. Chen, *ACS Catalysis*, **2015**, *5*, 3779-3785.

[16] A.M. Gómez-Marín, R. Rizo, J.M. Feliu, *Beilstein J. Nanotechnol*., **2013**, *4*, 956–967.

[17] E.L. Goldstein, M.R. Van de Mark, *Electrochim. Acta*, **1982**, *27*, 1079-1085.

[18] V. Climent and J.M. Feliu, *J. Solid State Electrochem.*, **2011**, *15*, 1297–1315.

[19] C.E. Hotchen, G.A. Attard, S.D. Bull and F. Marken, *Electrochim. Acta*, **2014**, *137*, 484-488.

[20] A. Rodes, K. El Achi, M. A. Zamakhchari and J. Clavilier, Fundamental Aspects of Heterogeneous Catalysis Studied by Particle Beams, 1990, Vol. 265 NATO ASI Series 75-82.

[21] T. Biegler, D.A.J. Rand and R. Woods, *J. Electroanal. Chem*., **1971**, *29*, 269.

[22] A. Rodes, M.J. Llorca, J.M. Feliu and J. Clavilier, *Anales Quimica*, **1996**, *92*, 118-127.

[23] J. Wang, D.F. Thomas and A. Chen, *Anal. Chem*., **2008**, *80*, 997-1004.

[24] N.M. Marković, H.A. Gasteiger, P.N. Ross, *J. Phys. Chem*., **1995**, *99*, 3411-3415.

[25] N.M. Marković, H.A. Gasteiger, P.N. Ross, *J. Phys. Chem.*, **1996**, *100*, 6715–6721.